AIP | The Journal of Chemical Physics

Communication: Nanosize-induced restructuring of Sn nanoparticles

Sareh Sabet and Payam Kaghazchi

Citation: The Journal of Chemical Physics **140**, 191102 (2014); doi: 10.1063/1.4878735

View online: http://dx.doi.org/10.1063/1.4878735

View Table of Contents: http://scitation.aip.org/content/aip/journal/jcp/140/19?ver=pdfcov

Published by the AIP Publishing

Communication: Nanosize-induced restructuring of Sn nanoparticles

Sareh Sabet[1] and Payam Kaghazchi[2,a)]
[1]*Institute of Materials Science, Technical University of Darmstadt, Alarich-Weiss-Strasse 2, 64287 Darmstadt, Germany*
[2]*Institut für Chemie und Biochemie, Freie Universität Berlin, Takustr. 3, 14195 Berlin, Germany*

(Received 16 March 2014; accepted 7 May 2014; published online 21 May 2014)

Stabilities and structures of β- and α-Sn nanoparticles are studied using density functional theory. Results show that β-Sn nanoparticles are more stable. For both phases of Sn, nanoparticles smaller than 1 nm ($\sim$48 atoms) are amorphous and have a band gap between 0.4 and 0.7 eV. The formation of band gap is found to be due to amorphization. By increasing the size of Sn nanoparticles (1–2.4 nm), the degree of crystallization increases and the band gap decreases. In these cases, structures of the core of nanoparticles are bulk-like, but structures of surfaces on the faces undergo reconstruction. This study suggests a strong size dependence of electronic and atomic structures for Sn nanoparticle anodes in Li-ion batteries. © *2014 AIP Publishing LLC*. [http://dx.doi.org/10.1063/1.4878735]

Tin (Sn) is an interesting anode material for Li-ion batteries (LiBs) owing to its high volumetric and gravitational capacities (993 mAh/g and 7200 mAh/cm^3).[1] The main problem in commercialization of LiBs with Sn anodes is large volume changes between delithiated phase (pure Sn) and fully lithiated phase ($Li_{4.4}Sn$).[2] This creates a large stress and strain, resulting in fracture and pulverization of the Sn anode and thus poor cycling ability.[3] One way out of this dilemma is using Sn-based nanostructures such as nanoparticles[4] and nanosheets.[5]

At temperatures lower than 13.2 °C, bulk Sn has a diamond structure, which is called α-Sn. Heating to higher temperatures under atmospheric pressure causes the α phase to transform into the β phase, which has a tetragonal structure.[6] The bulk properties of Sn such as lattice constant and cohesive energy as well as the $\alpha \rightarrow \beta$ phase transition have been extensively studied both experimentally and theoretically.[6–12] Many experimental efforts have also been devoted to study Sn nanostructures in LiBs,[13–15] but only few theoretical studies have addressed this subject.

Using density functional theory (DFT), we have recently studied incorporation of Li in Sn bulk and surfaces and found that β-Sn surfaces reconstruct in the presence of Li, while Li/α-Sn surfaces maintain their structures.[11] A recent combined experimental-theoretical investigation has also found that upon lithiation the structure of crystalline α-Sn is stable, while crystalline β-Sn becomes amorphous.[15]

In this Communication, using DFT calculations, we studied the structure of clean Sn nanoparticles of different shapes and sizes (between 0.5 and 2.4 nm) and found that nanoparticles smaller than 1 nm are amorphous-like and have a band gap greater than 0.4 eV. Larger nanoparticles are bulk-like/reconstructed core-shell nanoparticles and have no band gap.

The DFT calculations were performed using the SeqQuest code[16] with localized basis sets represented by linear combinations of contracted Gaussian functions and norm-conserving pseudopotentials. The results discussed in the paper are mainly based on the generalized gradient approximation (GGA) exchange-correlation functional proposed by Perdew, Burke, and Ernzerhof (PBE).[17] In order to investigate the sensitivity of our results on choosing a different exchange-correlation functional, we additionally recalculate the energetics and structures of β-Sn nanocubes with the local density approximation (LDA). To model the nanoparticles we used a 37 Å × 37 Å × 37 Å unit cell with at least 13 Å of vacuum spaces between images. Integrations in reciprocal space of Sn nanoparticles were performed at gamma point.

The β phase of Sn has a tetragonal structure (141 I41/amd), while the α phase of Sn has a diamond structure (227 FD-3M). The $\alpha \rightarrow \beta$ phase transition is accompanied by a large reduction of volume and the material transforms from a zero band gap semiconductor to a metal. The bulk properties such as the lattice constants, cohesive energies, and band gaps calculated using PBE and LDA are listed in Table I. We find that the lattice constants determined with PBE and LDA are in good agreement with the experimental values. However, the calculated cohesive energy of 3.19 eV with PBE functional is much closer to the experimental value of 3.12 eV than that of 4.00 eV with LDA functional. Our GGA-PBE and LDA calculations show no band gap for α-Sn, which is in agreement with experimental measurements. The calculated band gaps for α-Sn are 0.2 eV and 0.22 eV with HSE and HSEsol, respectively.[21]

Using the theoretical lattice constants we constructed clean β- and α-Sn nanoparticles of different shapes and sizes. The initial atomic positions in all Sn nanoparticles corresponded to those in the Sn bulk. For β-Sn, we focus on nanocubes consisting of {100} and {001} facets and sharp edges as well as nanospheres consisting of {100} and {001} facets and wide edges. Figure 1 shows the structures of Sn nanoparticles and their average binding energy with respect to the cohesive energy of Sn (E_b/E_c).

Our calculations for β-Sn nanocubes show that independent of the functional E_b/E_c increases with number of atoms. However, the calculated values of E_b/E_c is lower with LDA

a)payam.kaghazchi@fu-berlin.de

TABLE I. Lattice constants (Å), cohesive energies (eV), and band gaps (eV) for β-Sn and α-Sn bulk. Corresponding experimental values are given for comparison.

		Lattice constant	Cohesive energy	Band gap
β-Sn	PBE	$a = b = 5.96$, $c = 3.22$	3.13	0.00
	LDA	$a = b = 5.82$, $c = 3.15$	3.98	0.01
	Expt.	$a = b = 5.83126$, $c = 3.18141$[18]	...	0
α-Sn	PBE	$a = b = c = 6.64$	3.19	0.00
	LDA	$a = b = c = 6.48$	4.00	0.00
	Expt.	$a = b = c = 6.4798$[19]	3.12[20]	0

functional, which is due to the fact that this functional underestimates the stability of surfaces.[22] By enlarging the Sn nanoparticles (decreasing the surface contributions) the difference between LDA and PBE decreases. By fitting the calculated values of E_b/E_c, we estimate the critical size above which the surface contribution to the energy of nanoparticles is negligible, which gives $N_{Sn} = 10^7$ atoms or ~70 nm. This result is independent of choosing LDA or PBE. The structures of β-Sn nanocubes determined with LDA and PBE are also very similar. Thus, we only use the PBE functional for calculating the structures and energies of β- and α-Sn nanospheres.

For β-Sn nanospheres, we also find that E_b/E_c increases with size. Moreover, binding energies are very similar to those of β-Sn nanocubes.

Analysis of the structures shows that the β-Sn nanocubes of 0.5 and 0.8 nm (24 and 48 Sn atoms) are amorphous-like. Such an amorphization at zero-temperature zero-pressure conditions without any external parameter has not been reported so far in other metal nanoparticles. Although the degree of crystallization in the core of nanoparticles increases with size, the surface atoms are displaced from their bulk-terminated positions even in the largest studied nanoparticles (448 atoms). Figures 1(d) and 1(e) show structures of bulk-truncated and energetically minimized-geometrically-optimized nanoparticles. We find that the (100) and (001) surfaces are reconstructed. In particular, the low-coordinated Sn atoms at corners and edges are significantly displaced.

In order to distinguish between crystalline and amorphous structures, we compare radial distribution functions (RDFs), $g(r)$, of the Sn bulk with those of Sn nanoparticles. The calculated RDFs of the β-Sn bulk and nanocubes are illustrated in Fig. 2. The Sn–Sn bond lengths are shorter with LDA functional, which is in line with the calculated smaller lattice constants of Sn with LDA compared to PBE. The RDF of the Sn nanocube with size of 0.5 nm (24 atoms) is considerably different than that of the Sn bulk since it shows a variety of peaks which are absent in the RDF of the Sn bulk. However, by increasing the size of nanocubes the first RDF peak representing the first nearest neighbors becomes narrower and the other peaks that are not present in the Sn bulk disappear, which show a tendency to crystallization of Sn nanocubes. These results are again independent of using PBE or LDA. The deviation of the RDF in β-Sn nanocubes from that in the β-Sn bulk is found to be due to the surface reconstructions.

Afterwards, we study α-Sn nanospheres. Because of the computational demands for large unit cells, we considered nanospheres smaller than 2.1 nm. Figure 3 shows that,

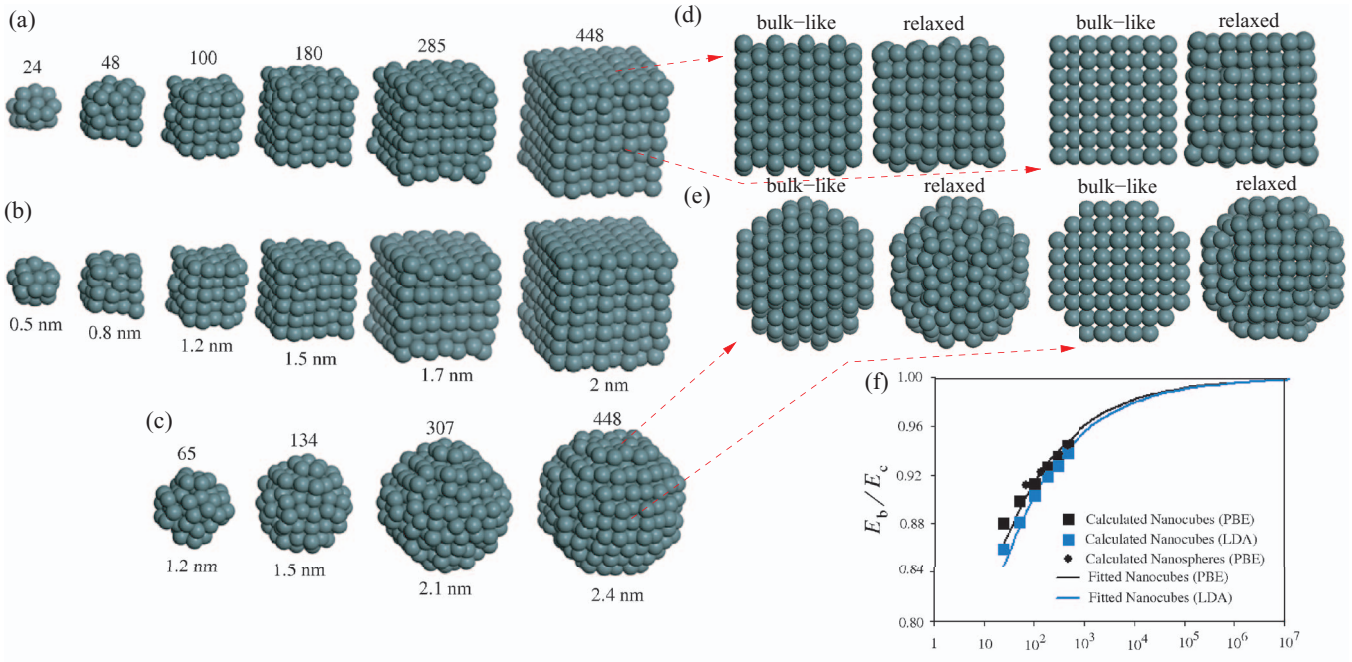

FIG. 1. Structures of β-Sn nanocubes calculated with the (a) PBE and (b) LDA functional as well as (c) structures of β-Sn nanospheres calculated with PBE. The top and front views of initial (bulk-like) and final (relaxed) structures of the largest studied (d) nanocube and (e) nanosphere calculated with PBE. (f) Binding energy per atom in the nanoparticles with respect to that in bulk (E_b/E_c) as a function of number of Sn atoms of the nanoparticles.

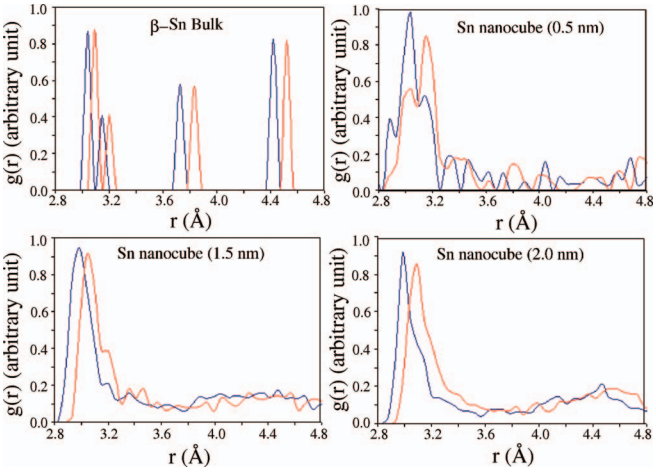

FIG. 2. Radial distribution functions $g(r)$ for β-Sn bulk and nanocubes calculated with the PBE (red solid lines) and LDA (blue solid lines) functional. We used intervals of 0.2 Å.

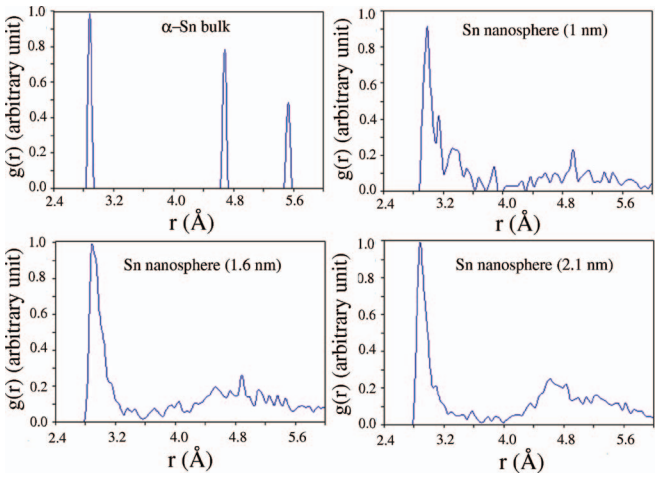

FIG. 4. Radial distribution functions g(r) for α-Sn bulk and nanospheres calculated with the PBE functional. We used intervals of 0.2 Å.

similar to the case of β-Sn, E_b/E_c increases with number of atoms. The smallest studied nanosphere with size of 1 nm (30 atoms) is amorphous-like. The degree of crystallization in the core of the α-Sn nanospheres increases with size, but even for the largest studied nanosphere (172 atoms, 2.1 nm) the surface atoms are considerably displaced due to their dangling bonds. Thus, the increase of E_b/E_c (Fig. 3) cannot be fitted with a similar function used for β-Sn (Fig. 1). A comparison between Figs. 1 and 3 shows that β-Sn nanoparticles are more favorable than α-Sn ones. Although this result is based on zero-temperature DFT calculations, we predict that, independent of temperature, β-Sn nanoparticles are always more stable. This is because previous DFT calculations for bulk β- and α-Sn have found that the vibrational entropy is smaller in α-Sn.[8]

The calculated RDFs (Fig. 4) show that, similar to the case of β-Sn, geometry optimization of small α-Sn nanospheres ($\leq$1 nm) leads to the formation of amorphous-like nanospheres and the larger nanospheres have more crystalline character.

Finally, we calculate band gap for β- and α-Sn nanoparticles (Fig. 5) and find that small nanoparticles consisting of 48 atoms and less have a band gap (HOMO–LUMO gap) between 0.4 and 0.7 eV. The band gap is due to the amorphization of Sn nanoparticles since the band gap is zero for the bulk-truncated structures (without geometry optimization). Previous DFT studies show that nonhybrid functionals such as PBE and LDA always underestimate band gaps of materials.[23] For example, the calculated band gaps using PBE and LDA for C are 1.31 and 1.25 eV lower than the experimental value of 5.48 eV, respectively. For Si, the underestimations of the band gap from the experimental value of 1.17 eV are 0.42 and 0.58 eV, respectively.[23] Therefore, the real band gap for Sn nanoparticles consisting of <48 atoms may be even larger than 0.4–0.7 eV.

In summary, our DFT calculation shows a size-dependent atomic structure and band gap in β- and α-Sn nanoparticles. It is found that nanoparticles with size of $\leq$1 nm are amorphous-like with band gaps larger than 0.4 eV, while larger nanoparticles with size of 1–2.4 nm are bulk-like/reconstructed core-shell with no band gap.

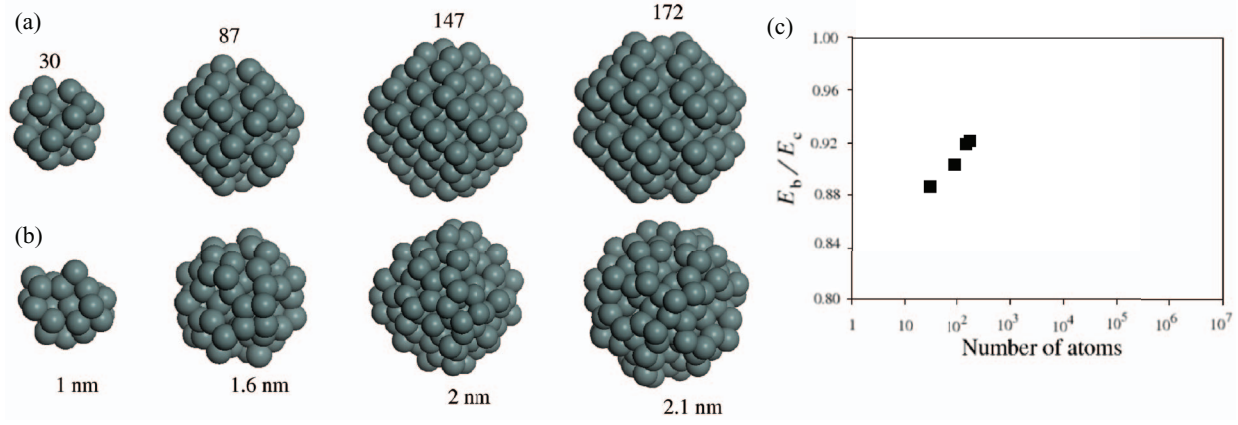

FIG. 3. Structures of (a) initial and (b) relaxed α-Sn nanospheres calculated with the PBE functional as well as (c) average binding energy of Sn atoms in α-Sn nanoparticles with respect to that in Sn bulk (E_b/E_c) as a function of number of atoms.

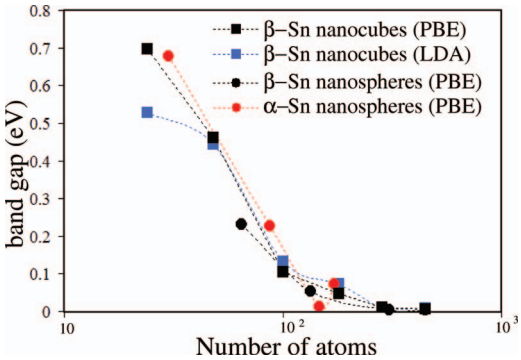

FIG. 5. Band gap as a function of number of Sn atoms for the Sn nanoparticles presented in Figs. 1 and 3.

The authors gratefully acknowledge support from the "Bundesministerium für Bildung und Forschung" (BMBF).

[1]D. Deng, M. G. Kim, J. Y. Lee, and J. Cho, Energy Environ. Sci. **2**, 818 (2009).
[2]L. Y. Beaulieu, K. W. Eberman, R. L. Turner, L. J. Krause, and J. R. Dahn, Electrochem. Solid-State Lett. **4**, A137 (2001).
[3]K. E. Aifantis and J. P. Dempsey, J. Power Sources **143**, 203 (2005).
[4]C. Kim, M. Noh, M. Choi, J. Cho, and B. Park, Chem. Mater. **17**, 3297 (2005).
[5]C. Wang, Y. Zhou, M. Ge, X. Xu, Z. Zhang, and J. Z. Jiang, J. Am. Chem. Soc. **132**, 46 (2010).
[6]A. Busch and R. Kern, Solid State Phys. **11**, 1 (1961).
[7]R. Ravelo and M. Baskes, Phys. Rev. Lett. **79**, 2482 (1997).
[8]P. Pavone, S. Baroni, and S. de Gironcoli, Phys. Rev. B **57**, 10421 (1998).
[9]P. Haas, F. Tran, and P. Blaha, Phys. Rev. B **79**, 085104 (2009).
[10]P. Kaghazchi, J. Chem. Phys. **138**, 054706 (2013).
[11]P. Kaghazchi, J. Phys.: Condens. Matter **25**, 382204 (2013).
[12]A. Aguado, Phys. Rev. B **67**, 212104 (2003).
[13]Y. Yu, L. Gu, C. Zhu, P. A. van Aken, and J. Maier, J. Am. Chem. Soc. **131**(44), 15984 (2009).
[14]Y. Zou and Y. Wang, ACS Nano **5**(10), 8108 (2011).
[15]H. S. Im, Y. J. Cho, Y. R. Lim, C. S. Jung, D. M. Jang, J. Park, F. Shojaei, and H. S. Kang, ACS Nano **7**(12), 11103 (2013).
[16]C. Verdozzi, P. A. Schultz, R. Q. Wu, A. H. Edwards, and N. Kioussis, Phys. Rev. B **66**, 125408 (2002).
[17]J. P. Perdew, K. Burke, and M. Ernzerhof, Phys. Rev. Lett. **77**, 3865–3868 (1996).
[18]E. R. Jette and F. Foote, J. Chem. Phys. **3**, 605 (1935).
[19]R. Farrow, D. Robertson, G. Williams, A. Cullis, G. Jones, I. Young, and P. Dennis, J. Cryst. Growth **54**, 507 (1981).
[20]W. Harrison, *Electronic Structure and the Properties of Solids* (Dover, New York, 1989).
[21]L. Schimka, J. Harl, and G. Kresse, J. Chem. Phys. **134**, 024116 (2011).
[22]P. Kaghazchi and T. Jacob, Phys. Rev. B **81**(7), 075431 (2010).
[23]J. Heyd, J. E. Peralta, G. E. Scuseria, and R. L. Martin, J. Chem. Phys. **123**, 174101 (2005).